Hindawi
Journal of Nanomaterials
Volume 2019, Article ID 7172641, 11 pages
https://doi.org/10.1155/2019/7172641

Research Article

Carbon Nanofibers Coated with Silicon/Calcium-Based Compounds for Medical Application

Wojciech Smolka,[1] Elzbieta Dlugon,[2] Piotr Jelen,[2] Wiktor Niemiec,[2] Agnieszka Panek,[3] Czeslawa Paluszkiewicz,[3] Barbara Zagrajczuk,[2] Elzbieta Menaszek,[4] Jaroslaw Markowski,[1] and Marta Blazewicz[2]

[1]*Clinical Department of Laryngology, Medical University of Silesia, School of Medicine, Katowice, Poland*
[2]*AGH University of Science and Technology, Faculty of Materials Science and Ceramics, Krakow, Poland*
[3]*Institute of Nuclear Physics, Polish Academy of Sciences, Krakow, Poland*
[4]*Department of Cytobiology, Collegium Medicum, Jagiellonian University, Krakow, Poland*

Correspondence should be addressed to Marta Blazewicz; mblazew@agh.edu.pl

Received 16 September 2018; Accepted 2 December 2018; Published 1 April 2019

Academic Editor: Yu Dong

The aim of this work was to develop a method for the manufacture of carbon nanofibers in the form of mats containing silicon and calcium compounds with potential biomedical application. Carbon nanofibers (ECNF) were prepared from the electrospun polyacrylonitrile (PAN) nanofibers. The electrospun polymer nanofibers were heat treated up to 1000°C to obtain carbon nanofibers. The surface of ECNF was covered with a silica-calcium sol (ECNF+Si/Ca) by dip-coating technique followed by the stabilization process. Both types of carbon nanofibers, i.e., the as-received and covered with the sol, were tested to confirm their osteoconductive properties. Biological tests were performed, including genotoxicity, cytotoxicity, and alkaline phosphatase (ALP) activity. Morphology of adhering cells to nanofiber surface was described. The nanofibers were subjected to a bioactivity test in contact with SBF artificial plasma. Biological tests have revealed that the nanofiber-modified ECNF+Si/Ca in contact with osteoblast cells were biocompatible, and the level of cytotoxicity was lower compared to the control. The ALP activity of the modified nanofibers was higher than nonmodified nanofibers and indicates potential applications of such carbon materials in the form of mats as a substrate for bone tissue regeneration.

1. Introduction

Carbon nanofibers are of interest to many fields of applications, such as energy storage, fuel cells, electronics, and catalysis, as well as in environmental protection and medicine [1–4]. They are a product of carbonization of polymer nanofibers, which are often electrospun in the form of mats, membranes, or threads. This method allows obtaining, among others, polyacrylonitrile nanofibers, which are the most popular precursor of carbon nanofibers with controlled diameter and complex chemical composition. Depending on the type of nanofibrous precursor and the processing variables of the carbonization process, materials with diverse structure and different surface parameters can be obtained [5–7].

Polymer nanofibers due to their large specific surface resulting from high surface to volume ratio and small diameter may act as an extracellular matrix for tissue engineering. Such nanofibers in the form of porous mats can be used as membranes for reconstructive medicine, as substrates for bone and cartilage development in the posttraumatic tissues [8–12]. A key issue is the fact that these nanofibers possess diameters slightly different from those of the collagen fibrils of bone tissue. Carbon nanofibers, like polymer nanofibers, thanks to their physical properties, become candidates for many medical applications; these materials are considered to be used in the construction of biosensors and electrodes to stimulate the nervous system as well as for the manufacture of scaffolds for regenerative medicine. In the form of

nonwovens, membranes, or various kinds of nanocomposites, they can be used in many fields of medicine [13–19].

Carbon fibers can be modified at the level of the organic precursor by selecting the appropriate processing parameters, i.e., during the carbonization process of the precursor, and also by the chemical surface treatment of the carbon fibers themselves [20–22].

Carbon micro- and nanofibrous materials obtained by heat treatment of the polymer precursor (carbonization) at low temperatures (about 1000°C) integrate well with tissues and can undergo a slow oxidation in the biological environment, turning into organic forms that do not pose a threat to the body [23, 24]. Our research shows that both the micro and carbon nanofibers have a potential in the treatment and regeneration of the cartilage [25, 26].

Fibrous implants made from nanofibers can also be candidates for applications in laryngology. This field particularly needs to develop a new generation of implants, whose wider use could contribute to a reduced number of operations using patient tissue. In laryngology, biomaterials are used in the ossicles, the reproduction of the posterior wall of the external auditory canal, the electrodes for cochlear implants, the reconstruction of the craniofacial elements, in nasal reconstructive surgery, and nasal septum [27–33]. Therefore, in this field, there is a need for materials with osteogenic and chondrogenic potential, as well as materials for the construction of medical electrodes. Low carbonized carbon nanofibers may be a valuable substrate, on the surface of which bioactive molecules and organic and inorganic substances can be introduced. The open microstructure of carbon nanofibers, devoid of the high-ordered near surface region characteristic for carbon microfibers, makes them exceptionally easy to modify not only limited to their surface. In our earlier studies, we modified carbon nanofiber surface with carbon and hydroxyapatite nanoparticles, thus preparing the nanofiber material for contact with bone tissue [34, 35]. Such modified nanofibers can be a starting point for the design and manufacture of materials intended for the treatment and regeneration of tissues.

A new approach of modifying carbon nanofibers is to cover the carbon structure with silicon-containing compounds. This allows obtaining a new bioactive biomaterial that can be used in osteochondral and bone tissue surgery.

The aim of the work was to develop a method for the modification of carbon nanofibers with silicon and calcium compounds for applications in bone regenerative medicine. Carbon nanofibers (ECNF) were prepared from the polyacrylonitrile precursor, and their surface was modified with a silica-calcium sol (ECNF+Si/Ca), functionalized in such way carbon nanofibers were tested to confirm their biocompatibility and osteoconductive properties. Biological tests were performed, including genotoxicity, cytotoxicity, and the alkaline phosphatase (ALP) activity. Morphology of adhering cells to nanofibers surface was described. The nanofibers were subjected to a bioactivity test in contact with SBF artificial plasma. So far, such approach to functionalize surface properties of carbon nanofibers has not yet been described in literature. The combination of carbon nanofibers doped with silica and calcium may be an interesting solution for the use in tissue therapy. The potential of this material in osteoblast cell culture is discussed.

2. Experimental

2.1. Material Preparation. Copolymer Mavilon Zoltek Company (Hungary) consisting of 93–94 wt% of acrylonitrile mers, 5–6 wt% of methyl acrylate mers, and approximately 1 wt% of sodium alilo-sulfonate mers was used to manufacture polymer nanofibers. The PAN nanofibers were spun from the polymer solution using the electrospinning method. The transformation of the polymer nanofibers into carbon nanofibers consisted of two steps. The first step was the stabilization, during of which the polymer nanofibers were oxidized in air at 250°C-300°C. The second step was annealing the oxidized samples in a nitrogen atmosphere, preventing oxidation of the nanofibers to 1000°C, at a heating rate of 5°C/min, without holding the samples at final temperature. Subsequently, the carbon nanofibers were subjected to a two-stage surface modification. In the first stage, the nanofibers were chemically treated with concentrated nitric acid at 60°C for one hour. Then, the carbon nanofibers were covered with a silica-calcium sol-gel solutions by dip-coating technique. The modifying medium was a mixture of two sols made on the basis of two precursors, i.e., tetraethoxysilane (TEOS) (Sigma-Aldrich product) and $Ca(NO_3)4H_2O$ (Sigma-Aldrich product). First, a silica sol was prepared by adding the TEOS to a determined volume of distilled water, ethyl alcohol 99.5%, and hydrochloric acid as a catalyst for the hydrolysis process. The sol was stirred at 50°C, for two hours. Then, the sol prepared from calcium nitrate and ethyl alcohol was added to the TEOS-based sol. The carbon nanofibers were then incubated in a mixture of sols for one hour, and subsequently, they were dried at 70°C, for 24 hours. The last step of the process was washing the nanofibers in distilled water and redrying. During this preparation, a thin polymer layer containing calcium and silicon atoms on the surface of the nanofiber was formed. More details of the preparation of the slurry sol and coating conditions on the nanofibers are described elsewhere [36, 37]. The following types of nanofibers were prepared for the study: the initial nanofibers (the as-received carbon nanofibers) denoted as ECNF (electrospun carbon nanofibers) and nanofibers modified with silica-calcium sol denoted as ECNF+Si/Ca. These samples were incubated in simulated body fluid (SBF) to determine their bioactivity. The incubated nanofibers in SBF were denoted as ECNF+HA [38].

2.2. Microscopic and Spectroscopic Study. The AFM measurements were conducted using the MultiMode VIII (Bruker) atomic force microscope in TappingMode (semicontact mode) using antimony-doped silicon probes with 8 nm nominal tip radius, 300 kHz cantilever resonance frequency, and 40 N/m spring constant. Infrared (FT-IR) spectra were recorded using a Bio-Rad FTS 165 spectrometer with a resolution of 2 cm^{-1} within the range of 4000-400 cm^{-1}. The morphology of the nanofibers was studied using the Nova NanoSEM 200 microscope connected to an EDAX EDS

point analyser. The obtained SEM images were analysed using the ImageJ freeware program, which measured the fibers' diameters. Using the segmental method, the overall porosity of the samples in the form of mats from the SEM microphotographs was determined.

2.3. In Vitro Biological Studies. Prior to biological testing, samples of carbon mats in the form of discs (12 mm in diameter) were washed in 70% ethanol and sterilized under UV-C light for 30 min on each side. For estimation of potential genotoxicity of the samples (ECNF, ECNF+Si/Ca), the normal human skin fibroblasts from cell line CCL-110 (American Type Culture Collection, ATCC) were used. The cells were cultured in MEM medium at 37°C and 5% CO_2. The studied nanomaterials (7.5 mg/4 ml PBS) were mixed by means of the ultrasonic probe (Palmer Instruments) for 2 min. Nanomaterial's suspension (500 μl) was added to well containing cells in 2 ml culture medium. Fibroblasts were contacted with nanomaterials at 37°C for 1 h or 24 h; next, the cells were washed in PBS and analysed by the comet assay procedure. The analysis of DNA damage levels after *in vitro* treatment was performed using the alkaline version of the comet assay [39, 40].

The suspension of *in vitro* treated fibroblasts was embedded in agarose on microscope slides. The cells and nuclear membranes were then lysed for 1 h in the agarose by detergent (1% Triton X-100) in alkaline pH > 13. Next, the DNA was subjected to alkaline electrophoresis (30 min, 4°C, 30 V, and 300 mA). After ethidium bromide (17 mg/ml) staining of cells, cellular DNA was visualized using the epifluorescence microscope Olympus BX-50 (Olympus, Tokyo, Japan). For the analysis of the comet pictures, the Komet 3.0 program from the Kinetic Imaging Company (Liverpool, UK) was used. DNA damage was quantified by the T-DNA (tail DNA) (DNA percentage in the comet tail), where the changes in the distribution of tail DNA are considered as a sensitive indicator of initial DNA breakage and DNA repair. Two independent experimental replicates were performed for each aliquot; 200 cells were analyzed for each data point (2 slides per dose, 100 cells analysed from each slide). The data were presented as mean values and standard error. The statistical analysis was performed using the Student t -test from Excel software. The p values equal to or less than 0.05 were considered significant.

Besides genotoxicity study and cytotoxicity tests including cell viability, ALP levels were carried out with bone cells. The cell morphology assessment after contact with carbon nanofiber mats was also determined. The normal human osteoblast cells (NHOst; Lonza, USA) were expanded in 75 cm^2 tissue culture flasks (Nunc™, Denmark) in the osteoblast growth medium (OGM™; Lonza, USA) supplemented with 10% fetal bovine serum (FBS; Lonza, USA), 0.1% ascorbic acid (Lonza, USA), and 0.1% gentamicin (GA-1000; Lonza, USA), at 37°C in a humidified, 5% CO_2 atmosphere. Medium was changed every 3 days until a 70% confluent cell monolayer was developed. Then, cells were detached from culture flasks using 5% trypsin-EDTA (HyClone, USA). The prepared sterile thin films were then placed at a bottom of 48-well culture plate wells (Nunc™, Denmark) and held by polycarbonate inserts (Scaffdex, Finland) to prevent the samples from floating. The cells were seeded on the material surface at a density of $2{\cdot}10^4$ cells/ml/well and cultured for 3 and 7 days. The bottom surface of tissue culture polystyrene (TCPS) wells served as a positive control. The cells were cultured in the differentiating conditions in the osteoblast growth medium (OGM™, Lonza, USA) supplemented with 200 nM hydrocortisone-21-hemisuccinate (Lonza, USA) and 10 mM β-glycerophosphate (Lonza, USA). In order to determine the number of NHOst cells and cytotoxic effect of obtained materials after 3 and 7 days of culture, ToxiLight™ BioAssay Kit and ToxiLight™ 100% Lysis Reagent Set (Lonza, USA) were used. The kit was used to quantify adenylate kinase (AK) in both supernatant (representing damaged cells) and cell lysate (representing intact adherent cells). Luminescence was measured using a microplate reader POLARstar Omega (BMG Labtech, Germany). The results were expressed as mean ± standard deviation (SD) from 8 samples for each experimental group. The alkaline phosphatase (ALP) activity was determined using 4-methylumbelliferyl phosphate (4-MUP). ALP cleaves the phosphate group of the nonfluorescent 4-MUP substrate into the soluble highly fluorescent substance methylumbelliferone. The hydrolysis of MUP was determined by fluorescence detection on a POLARStar Omega microplate reader (BMG Labtech, Germany) with settings for excitation at 360 and emission at 440 nm. The ALP activity was measured as relative fluorescence units (RFUs) after 3, 7, and 21 days of culture. Besides the ALP test, bioactivity of ECNF+Si/Ca samples was evaluated by the microscopic analysis of the samples before and after maintaining them in SBF at 37°C, for 3 and 10 days.

For evaluation of the cells' morphology and their attachment to the fibrous biomaterials, the cell cultures were stained with 0.01% acridine orange (AO) solution (Sigma-Aldrich, Germany) for 1 min, washed in PBS, and observed under the fluorescence microscope Olympus CX41 (Japan). Photographic documentation was made by the E-520 camera (Olympus, Japan).

3. Results and Discussion

3.1. Characterization of Carbon Nanofibers. Figure 1 shows SEM images of three types of carbon nanofibers with EDS analysis, i.e., initial nanofibers, modified in a silica-calcium sol and the nanofibers after incubation in SBF for 3 and 14 days.

The SEM microphotographs of ECNF show randomly oriented nanofibers creating a mat about 50 nm thick (Figure 1(a)). The average parameters characterizing nanofibrous samples are collected in Table 1.

The overall porosity of the fibrous samples is ranging between 0.47 and 0.76, depending on the type of samples (Table 1). Since biomaterials for tissue engineering purposes should have high porosities enabling cell culture, this parameter seems to be favourable for such applications. Carbon nanofibers obtained by the carbonization of the polyacrylonitrile precursor form a 3D isotropic system with different diameters ranging from 150 to 300 nanometers, with a mean diameter of 190 nm. The modification in the SiO-Ca sol does not change

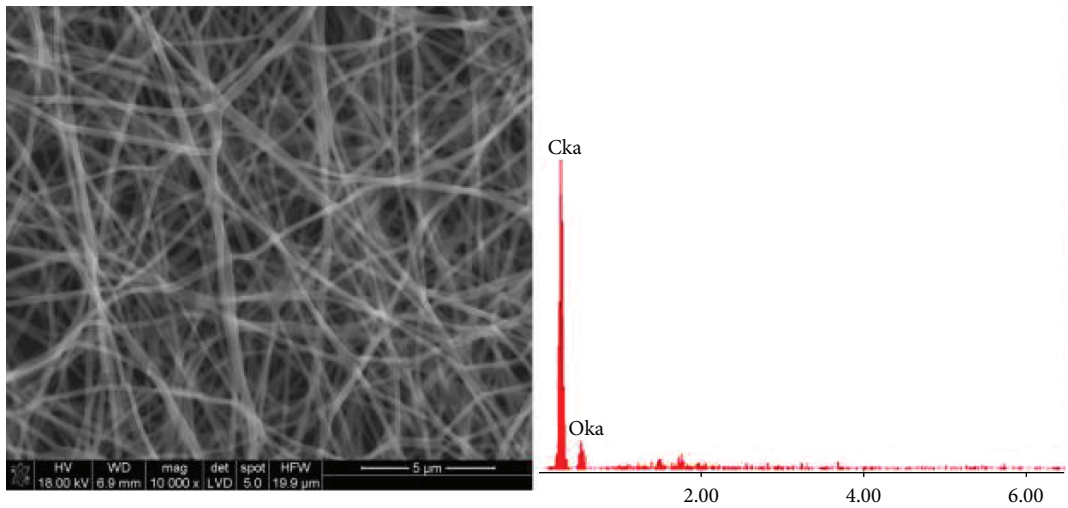

(a)

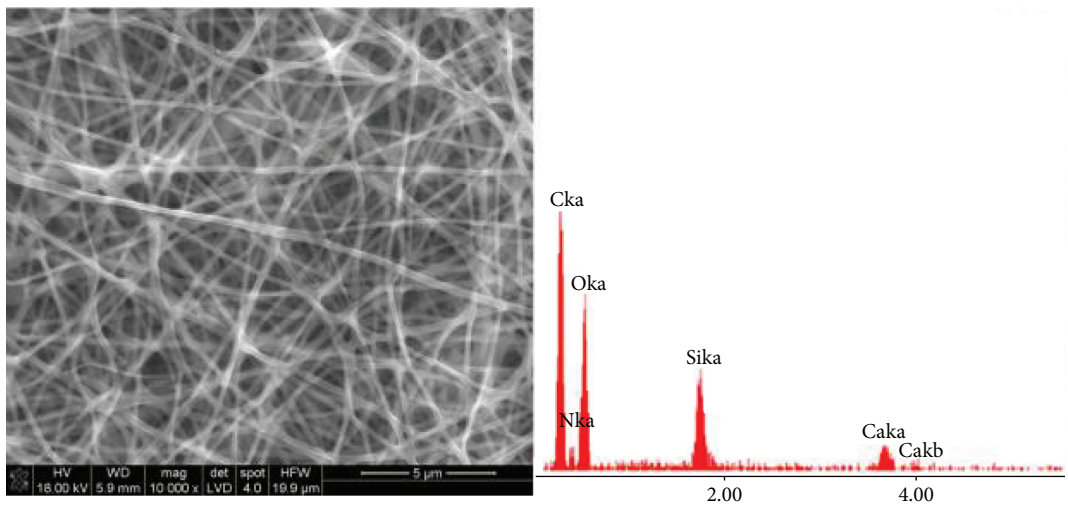

(b)

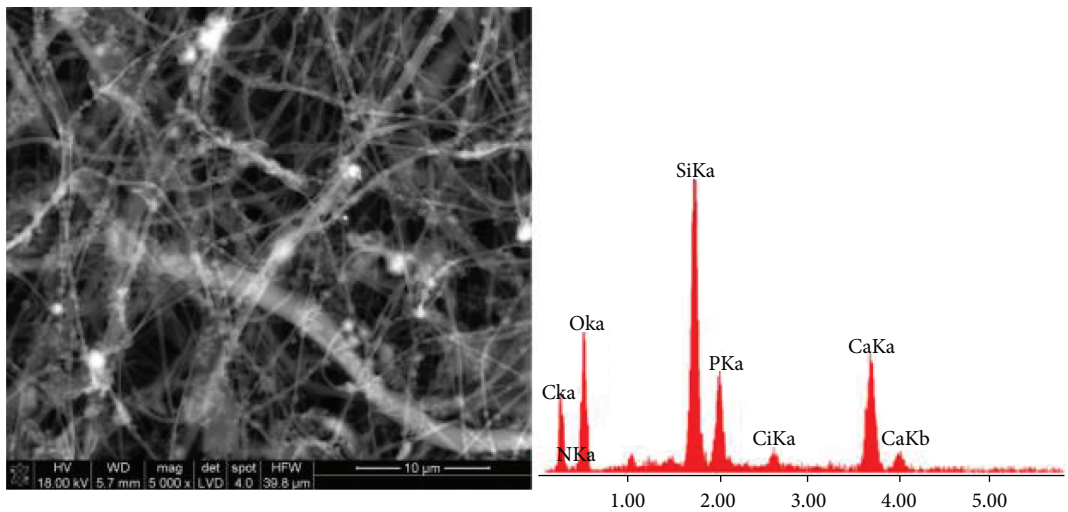

(c)

Figure 1: Continued.

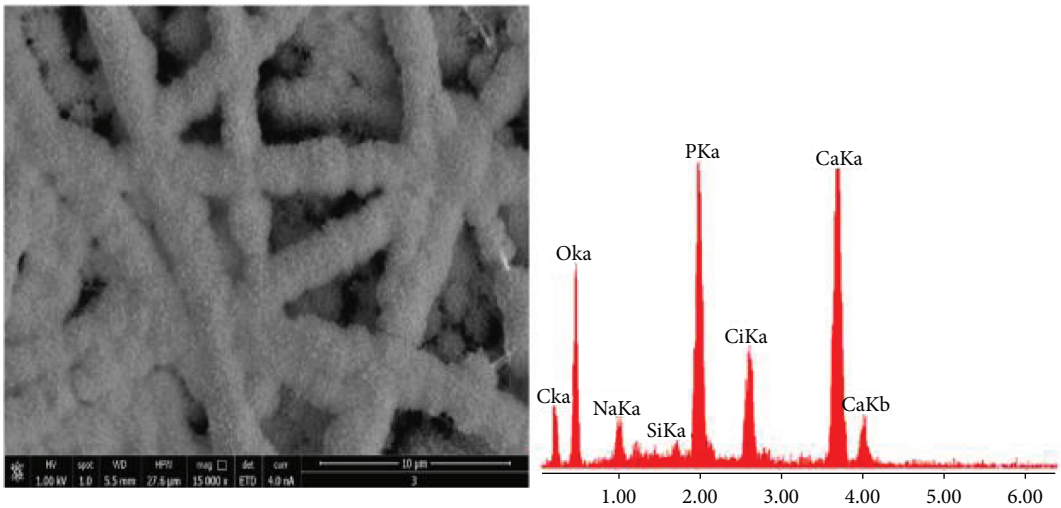

(d)

Figure 1: SEM images with EDS analysis of (a) ECNF and (b) ECNF-Si/Ca nanofibers functionalized in SiO_2-CaO sol (c) after 3-day incubation and (d) after 14-day incubation in SBF.

Table 1: Microstructure parameters of nanofibrous mats.

Type	Fiber diameter, d (nm)	Material porosity, p
ECNF	190 ± 27	0.76 ± 0.02
ECNF+Si/Ca	231 ± 34	0.71 ± 0.02
ECNF+HA	1234 ± 112	0.47 ± 0.03

distinctly the morphology of the fibrous mats, whereas the diameter of individual nanofibers increases ranging from 190 to 420 nanometers. The three-day incubation of nanofibers covered with the ceramic layer in SBF causes a number of needle-like precipitates to appear on their surface. Prolonging the incubation to 14 days in SBF makes the surface of the nanofibers completely covered with a layer of tightly adherent new phase forming a fibrous carbon-ceramic system with a characteristic nanotopography. The mean diameter of nanofibers in the mat after the 14-day incubation increases up to about 1200 nm. Figure 2 shows images of the nanofibers made by means of AFM.

The X-ray point microanalysis, EDS, shows the differences in the elemental composition of all types of nanofibrous mats. After the oxidative pretreatment, on the surface of the nanofibers (ECNF), only oxygen is present, in addition to carbon, while their treatment in the SiO_2-CaO sol causes the appearance of the bands in the spectrum corresponding to the presence of silicon and calcium. The infrared spectrum of CNF+Si/Ca samples incubated in SBF for 3 days contains, in addition to the strong bands attributed to the presence of oxygen and silicon, also bands associated with the presence of phosphorus and calcium. Such bands are not observed in the initial carbon mat (ECNF).

A 14-day incubation leads to the formation of two intense bands brought about the presence of phosphorus and calcium, whereas the remaining bands, especially those attributed to silicon or carbon, have a low intensity.

FTIR spectra of samples are shown in Figure 3.

The initial carbon nanofibrous mats (1) obtained by the carbonization of the PAN precursor (ECNF) are characterized by a relatively low degree of structural ordering, typical for the turbostratic carbon structure, in which strongly defected crystallites occur [41]. The infrared spectrum of such nanofibers is characterized by carbon crystallites containing heteroatoms including oxygen, hydrogen, and nitrogen, as evidenced by a broad-band boundary corresponding to the single carbon bonding with oxygen, hydrogen, and nitrogen. The band at 1574 cm^{-1} is attributed to vibrations of C=C bonds. The immersion of the ECNF in the silica-calcium sol changes the spectrum of carbon nanofibers (2). Bands present in the spectrum indicate the formation of a silicon-oxygen layer on the nanofiber surfaces. Characteristic bands for this structure occur at 462 cm^{-1} (-Si-O-Si bending), 802 cm^{-1}, the band corresponding to not fully condensed silica network O-Si-O, and the band at 1090 cm^{-1} assigned to –O-Si stretching vibrations. The spectrum also shows the bands associated with the organic component, i.e., stretching vibrations of bonds in which the silicon forms the bonds in hydrocarbon systems at 1200-1400 cm^{-1} and 2880-2900 cm^{-1}. The band at about 1130 cm^{-1} (the inflexion clearly visible on the band edge at 1090 cm^{-1} band) may indicate the formation of Si-O-C bonds. After 3-day incubation in SBF, in the spectrum (3) of nanofibers, low-intensity bands appearing in the range of 460-560 cm^{-1} indicate the presence of apatite on the sample surface [42, 43]. The spectrum contains bands indicating the presence of an amorphous phase associated with the presence of silicon-oxygen moieties on the sample surface. The wide envelope of the band, especially in the range between 800 and 950 cm^{-1}, may indicate the presence of silanol groups. It can be assumed that reaction between the groups containing oxygen and silicon in the incubation fluid environment leads to the formation of silanol groups that promote nucleation of apatite. It is known that the role of silicon is extremely

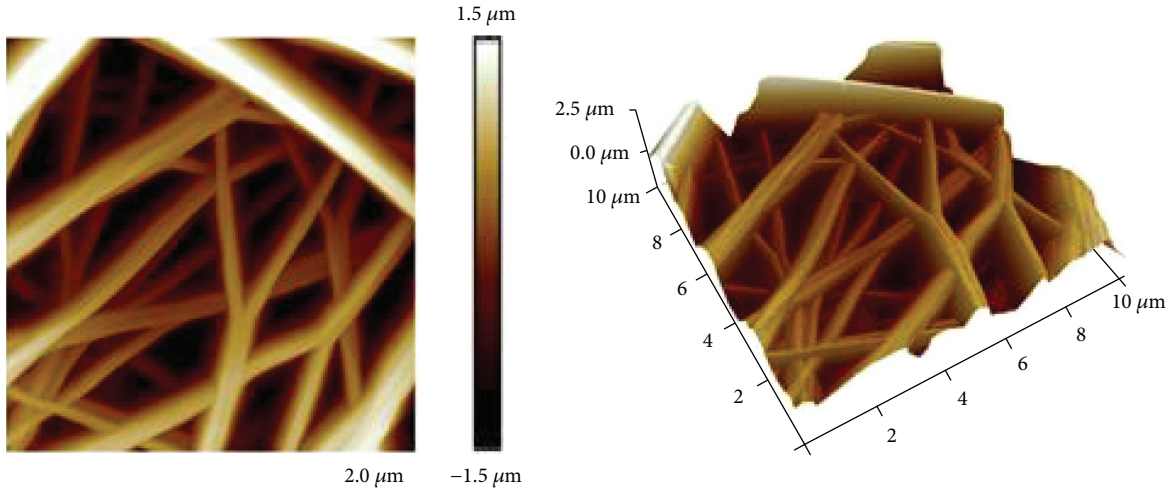

(a)

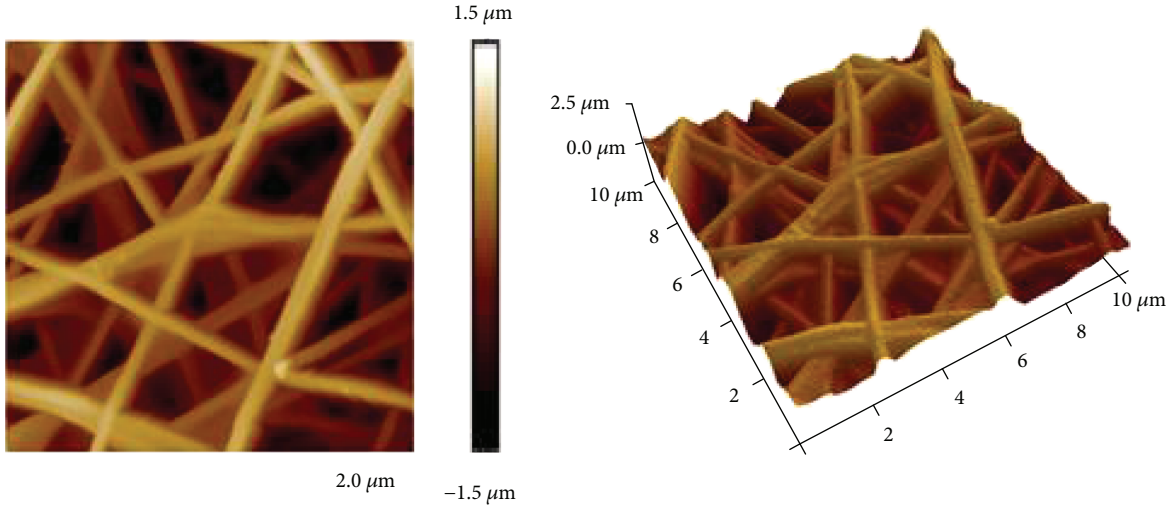

(b)

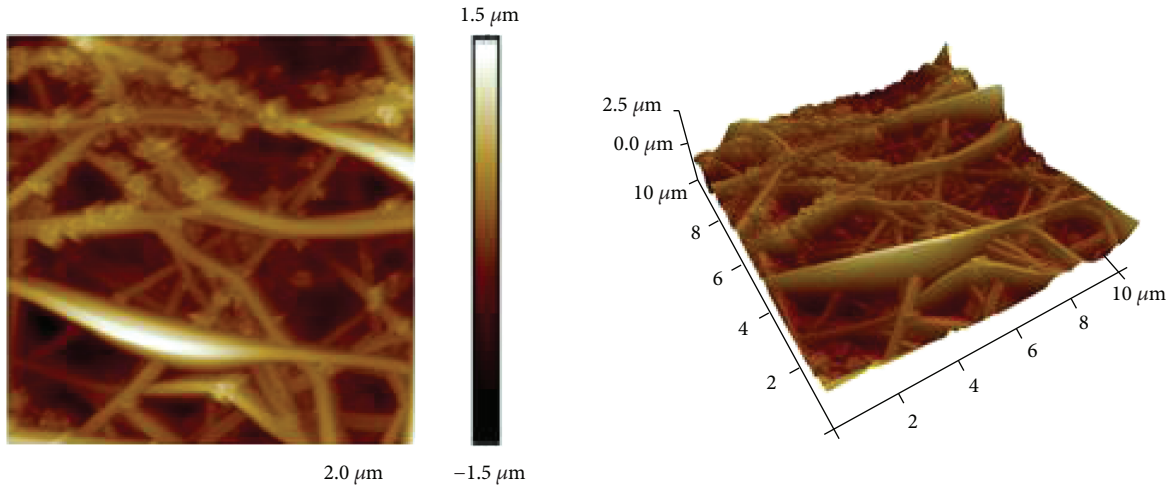

(c)

Figure 2: Continued.

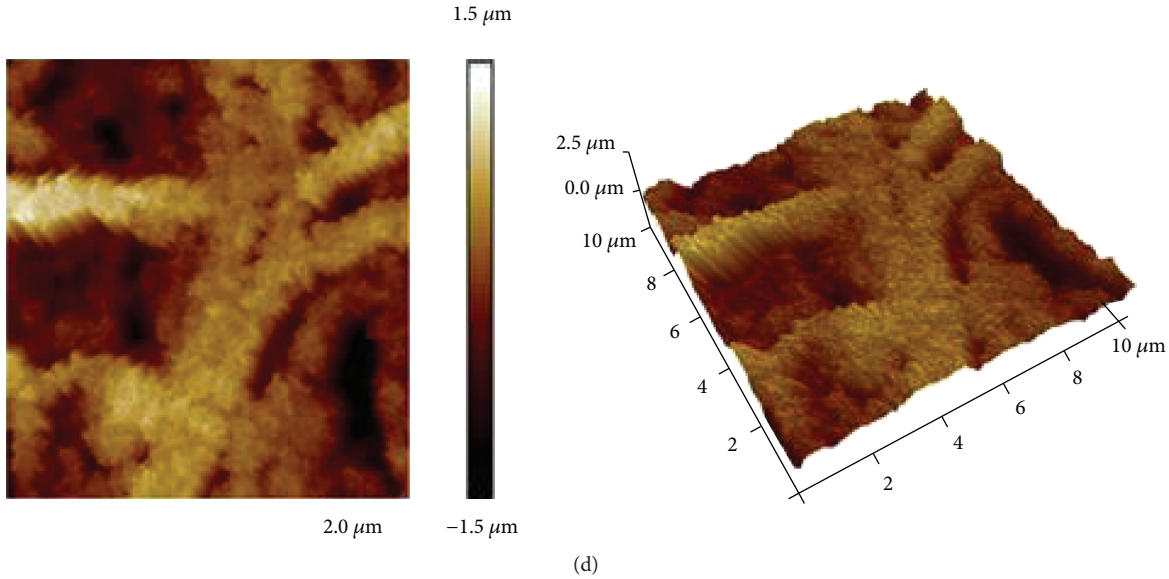

Figure 2: AFM images of (a) ECNF and (b) ECNF-Si/Ca functionalized nanofibers in SiO_2-CaO sol (c) after 3-day incubation and (d) after 14-day incubation in SBF.

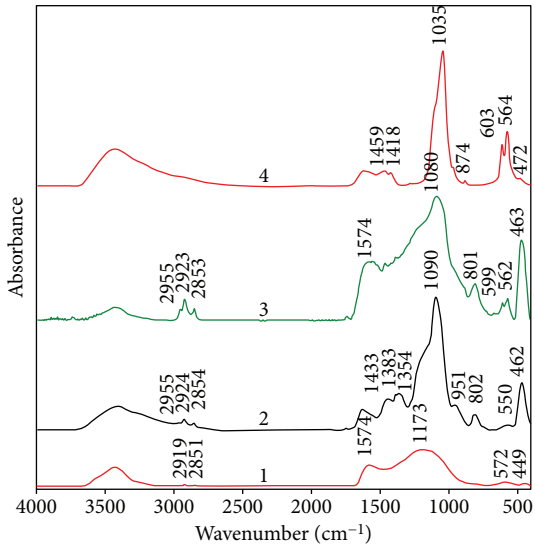

Figure 3: FTIR spectra of (1) initial nanofibers and (2) surface-functionalized nanofibers with Si/Ca sol and (3) after incubation in SBF 3 days and (4) two weeks.

important in the regeneration process of the osseous and connective tissues [44, 45]. The formation of silanol groups is accompanied by the transfer of calcium to the incubation solution, causing local saturation in the SBF environment. After the 14-day incubation of nanofibers, a solid layer of apatite appears on their surface and, in the spectrum, the bands (4) originating from silicon-oxygen groups become invisible. Bands in the area of 1400 cm^{-1} indicate that apatite containing carbonate groups is formed on the carbon surface.

The results obtained from microscopic and spectroscopic studies clearly indicate that the treatment of nanofibers in the silica-calcium sol leads to significant changes in the structure of their surface; as a result, it becomes the nucleation sites of apatite in contact with SBF.

Already after three days of interaction of the nanofiber surface with SBF, crystallites with the specific needle-shaped apatite crystallites having nanometric dimensions are visible (Figure 2). After longer incubation, the morphology of the apatite layer on the surface changes and the apatite needles connect to each other with their surfaces and completely cover the carbon surfaces to form a solid carbon-ceramic composition.

Biological tests are aimed at evaluating the samples' biocompatibility and bioactivity. Genotoxicity of the carbon nanofibers was assessed by means of the comet test, in terms of the tail DNA, and the results are collected in Table 2. The ECNF sample induces a significantly higher level of the DNA damage level in comparison to the control. After functionalization, however, these nanomaterials (ECNF-Si/Ca) are better tolerated by the cells and have significantly lower genotoxicity, comparable to the control.

The results of cytotoxicity test are presented in Figure 4.

Cell cytotoxicity of pure carbon mats determined on day 3 after seeding is higher compared to both ECNF+Si/Ca and control. On day 7 after cell seeding, a significant increase in cytotoxicity for initial carbon nanofibers can be observed. The difference is observed between both types of carbon mats and between the initial carbon mat and control. The modified carbon nanofibers are not cytotoxic for a short period of time (3 and 7 days) in NHOst cultures. The initial carbon nanofibers (ECNF) perform the highest percentage ratio of relative cytotoxicity compared to the control.

The cells' viability results of the sample materials are shown in Figure 5. The viability of both carbon nanofibers is compared to the control (TCPS). The number of cells cultured on ECNF+Si/Ca samples is comparable to the control and higher than that obtained for pure ECNF after 7 days of incubation.

Table 2: Genotoxicity of carbon mats in fibroblast cell line estimated by the t-DNA comet assay parameter.

	Control	ECNF	ECNF-Si/Ca
1 hour			
T-DNA	3.59 ± 0.21	8.51 ± 0.43	4.33 ± 0.32
Significance vs. control	—	0.00	0.24
24 hours			
T-DNA	3.32 ± 0.26	8.52 ± 1.05	6.27 ± 1.07
Significance vs. control	—	0.01	0.06

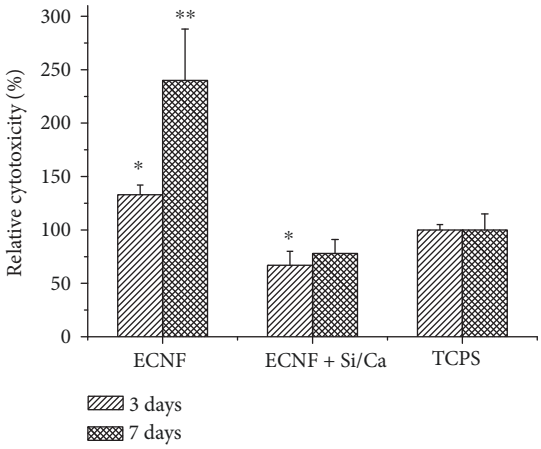

Figure 4: Material cytotoxicity for NHOst cultured on the surface of carbon samples; control was taken as 100%. *Statistically significant carbon samples on day 3 vs. TCPS ($p \leq 0.05$). **Statistically significant carbon samples on day 7 vs. TCPS ($p \leq 0.05$).

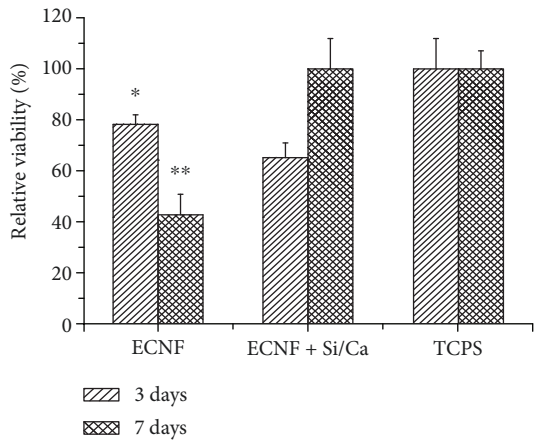

Figure 5: Viability of NHOst cultured in contact with carbon nanofibrous mats. *Statistically significant ECNF on day 3 vs. ECNF+Si/Ca and control ($p \leq 0.05$). **Statistically significant ECNF on day 7 vs. ECNF+Si/Ca and control ($p \leq 0.05$).

In vitro experiments reveal differences between the initial and modified nanofibers. Both tests indicate that the results are more favourable for the modified nanofibers compared to the initial ones. Experiments conducted by numerous workers have shown that the degree and methods

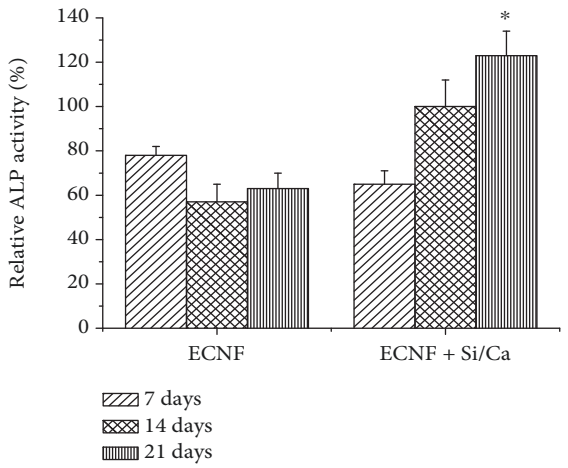

Figure 6: ALP activity in NHOst cells cultured on carbon nanofiber mats. *Statistically significant ECNF+Si/Ca on day 7 vs. ECNF ($p \leq 0.05$). **Statistically significant ECNF+Si/Ca on day 14 vs. ECNF ($p \leq 0.05$). ***Statistically significant ECNF+Si/Ca on day 21 vs. ECNF ($p \leq 0.05$).

of functionalization strongly affect carbon nanofiber cytotoxicity. In our experiments, the cells were incubated on electrospun mats for a relatively short time. Some effects could not have been visible while prolonging cell culture may reveal further differences in materials studied. The results of ALP activity are summarized in Figure 6.

There are statistical differences in the ALP activity between unmodified carbon mats and the mats containing silicon and calcium compounds (Figure 6). Already after 3 days, the test shows significant differences between both types of samples. The highest difference in ALP activity between the samples is noted on day 21 of the test; the RFU parameter for ECNF is about 50% higher compared to ECNF. These results indicate that additional surface functionalization of carbon nanofibers improves their osteoinductivity.

Fluorescence microphotographs displaying adhesion and morphology of osteoblasts on carbon samples cultured from 3 to 7 days are shown in Figure 7.

The analysis of the NHOst's morphology shows the cells covering uniformly and densely the materials' surfaces. These findings indicate that expanding cells on nanofibrous layers are not affected by the scaffold after 3 day culture. The shape of the cells is uniform and they are flattened, mostly well spread on the sample surfaces. The differences are observed in the number of cells between ECNF and ECNT+Si/Ca. The number of cells on unmodified ECNF is significantly lower in comparison with modified samples. Moreover, on the ECNF+Si/Ca sample, the numerous intercellular connections are observed, creating a dense cellular web (Figures 7(b) and 7(d)). For this sample, a certain directional arrangement of cells both after three and seven days of culture can also be observed, indicating the preferential direction of cell growth on the nanofibrous substrate. Such image is especially observed after longer time of cell culture on the ECNF+Si/Ca sample. Moreover, for the ECNF+Si/Ca sample, the cells form a lot of contacts with each other; they are well spread

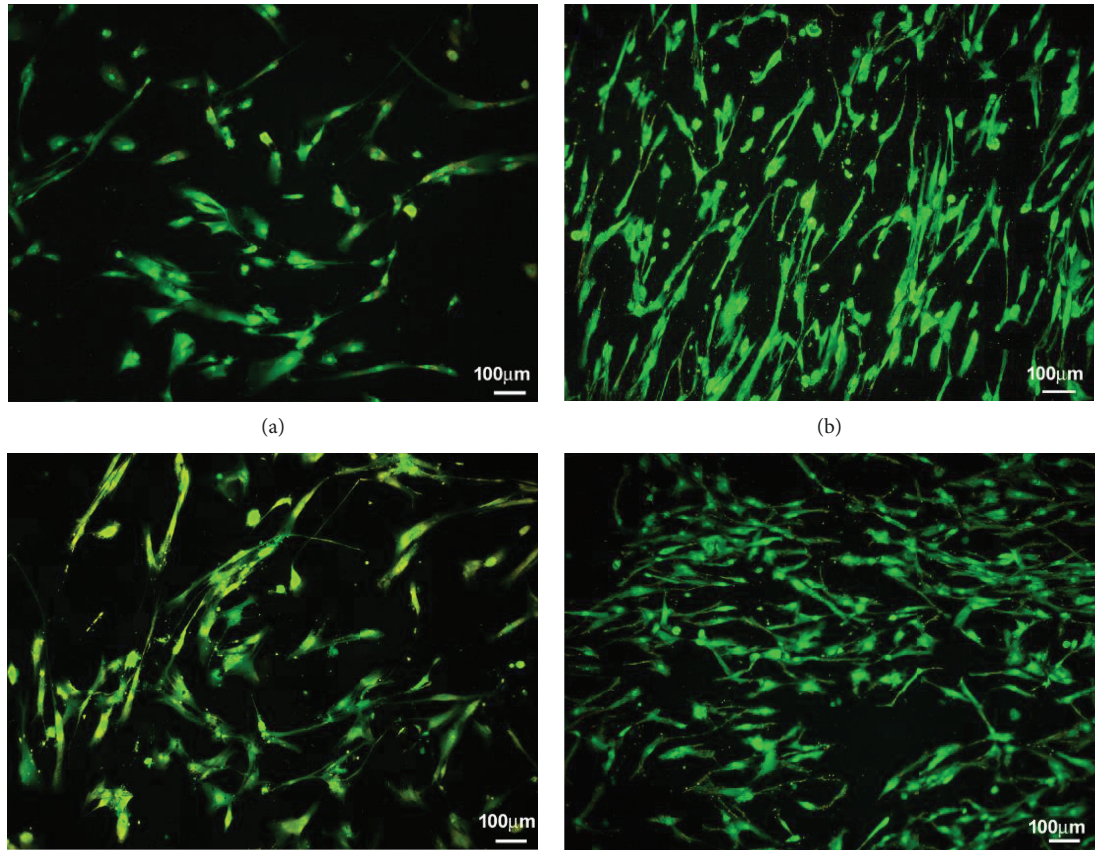

(a) (b) (c) (d)

Figure 7: Microphotographs of NHOst morphology cultured for (a, b) three days and (c, d) seven days on the surface of fibrous samples. (a, c) ECNF, (b, d) ECNF+Si/Ca (mag. 40x).

indicating the existence of a number of contact points between the cells and the substrate (Figures 7(b) and 7(d)).

A good cell adhesion to the surface is important factor in terms of further cellular functions such as proliferation, secretion, and production of the extracellular matrix. In the case of ECNF+Si/Ca mats, the cells additionally penetrated into the scaffolds' depth. This observation indicates that the modified nanofibers display a suitable 3-D architecture for cell culturing. A nanoscale size carbon mats have a relative high specific surface area and specific pore structure. The microstructure of carbon mats obtained in this work is characterized by high amount of interconnected open pores up to 76%, and the pore sizes are in micron scale (Figure 2) and expected to be large enough to allow cell adhesion and migration within the material space and to maintain the proper cell morphology. An optimal porosity and pore size of tissue supporting structure are important factors affecting migration of cells through the material. Additional functionalization of the carbon mat surface in which silanol groups are formed seems to be an effective way to obtain a biomaterial that can activate the regeneration of bone tissue due to the presence of silicon. Silicon is known to play a key role in improving bone regeneration and increasing bone mineral density.

Our biological tests are aimed at evaluating biocompatibility and bioactivity of the carbon samples in the form of mats. *In vitro* experiments show differences between unmodified (initial) and modified carbon nanofibrous materials. The tests indicate that the results are more favourable for the modified nanofibers compared to the initial nanofibers. In our experiments, the cells were incubated on electrospun mats for a relatively short time. Some effects could not have been visible, and prolonging cell culture can reveal further differences in materials studied.

One of the objectives of the surface modification of carbon nanofibers is to develop an active material that could be used to regenerate osteochondral tissue, e.g., for laryngology. The previous literature reports indicate that carbon materials, including carbon fibers and carbon nanotubes, may act as substrates with chondrogenic properties [25, 26]. Thus, the modified carbon nanofibers with a Si/Ca sol may be suitable substrates for osteochondral tissue.

4. Conclusions

A method for the surface modification of carbon nanofibers by impregnating them with the silica-calcium sol has been developed. It has been shown that the modified nanofibers with such treatment already after 3-day incubation in SBF activate the deposition of hydroxyapatite much stronger as compared to the unmodified carbon nanofibers. Prolonging the incubation to 14 days makes the surface of the

nanofibers completely covered with a hydroxyapatite layer of tightly adherent deposit forming a fibrous carbon-ceramic system with a characteristic nanotopography. Biological tests have revealed that modified carbon nanofibers (ECNF+Si/Ca) in contact with osteoblast cells were biocompatible, and the level of their cytotoxicity was lower compared to the control. ALP activity of the modified nanofibers was higher than unmodified nanofibers and indicates potential applications of such carbon materials in the form of mats as a substrate for bone tissue regeneration. Carbon nanofibers subjected to appropriate modifications may be a material with osteogenic properties.

Carbon nanofibers obtained by controlled heat treatment of the nanometric fibrous PAN precursor constitute a suitable material for the surface functionalization and can be considered as a useful material for fast and effective bone tissue regeneration. Moreover, such materials, due to their unique structure, can be valuable substrates to be modified by the use of the bioactive agents. Laryngology is a field of special interest for implants displaying both osteogenic and chondrogenic properties. Carbon micro- and nanofibers proved to have a potential in the treatment and regeneration of the cartilage. This fact combined with the possibility of the carbon material functionalization, and material combination indicates that such fibrous biomaterials may be a valuable constituent for the construction of materials for medical therapy and diagnostics, including laryngology.

Data Availability

The data used to support the findings of this study are available from the corresponding author upon request.

Conflicts of Interest

The authors declare that there is no conflict of interest regarding the publication of this paper.

Acknowledgments

This work has been supported by the Polish National Science Center (Grant no. UMO 2014/13/B/ST8/01195).

References

[1] L. Zhang, A. Aboagye, A. Kelkar, C. Lai, and H. Fong, "A review: carbon nanofibers from electrospun polyacrylonitrile and their applications," *Journal of Materials Science*, vol. 49, no. 2, pp. 463–480, 2014.

[2] L. Ji, Z. Lin, A. J. Medford, and X. Zhang, "Porous carbon nanofibers from electrospun polyacrylonitrile/SiO_2 composites as an energy storage material," *Carbon*, vol. 47, no. 14, pp. 3346–3354, 2009.

[3] L. Qie, W. M. Chen, Z. H. Wang et al., "Nitrogen-doped porous carbon nanofiber webs as anodes for lithium ion batteries with a superhigh capacity and rate capability," *Advanced Materials*, vol. 24, no. 15, pp. 2047–2050, 2012.

[4] J. Liu, S. Wang, J. Yang et al., "$ZnCl_2$ activated electrospun carbon nanofiber for capacitive desalination," *Desalination*, vol. 344, pp. 446–453, 2014.

[5] J. Liu, L. He, S. Ma, J. Liang, Y. Zhao, and H. Fong, "Effects of chemical composition and post-spinning stretching process on the morphological, structural, and thermo-chemical properties of electrospun polyacrylonitrile copolymer precursor nanofibers," *Polymer*, vol. 61, pp. 20–28, 2015.

[6] Z. Zhou, C. Lai, L. Zhang et al., "Development of carbon nanofibers from aligned electrospun polyacrylonitrile nanofiber bundles and characterization of their microstructural, electrical, and mechanical properties," *Polymer*, vol. 50, no. 13, pp. 2999–3006, 2009.

[7] C. Liu, Y. Feng, H. He, J. Zhang, R. Sun, and M. Chen, "Effect of carbonization temperature on properties of aligned electrospun polyacrylonitrile carbon nanofibers," *Materials & Design*, vol. 85, no. 15, pp. 483–486, 2015.

[8] M. M. Stevens, "Biomaterials for bone tissue engineering," *Materials Today*, vol. 11, no. 5, pp. 18–25, 2008.

[9] J. M. Holzwartha and P. X. Ma, "Biomimetic nanofibrous scaffolds for bone tissue engineering," *Biomaterials*, vol. 32, no. 36, pp. 9622–9629, 2011.

[10] W. J. Lia, R. Tulia, C. Okafora et al., "A three-dimensional nanofibrous scaffold for cartilage tissue engineering using human mesenchymal stem cells," *Biomaterials*, vol. 26, no. 6, pp. 599–609, 2005.

[11] E. J. Levorson, P. R. Sreerekha, K. P. Chennazhi, F. K. Kasper, S. V. Nair, and A. G. Mikos, "Fabrication and characterization of multiscale electrospun scaffolds for cartilage regeneration," *Biomedical Materials*, vol. 8, no. 1, article 014103, 2013.

[12] H. J. Shin, C. H. Lee, I. H. Cho et al., "Electrospun PLGA nanofiber scaffolds for articular cartilage reconstruction: mechanical stability, degradation and cellular responses under mechanical stimulation in vitro," *Journal of Biomaterials Science Polymer Edition*, vol. 17, no. 1-2, pp. 103–119, 2006.

[13] V. Vamvakaki, K. Tsagaraki, and N. Chaniotakis, "Carbon nanofiber-based glucose biosensor," *Analytical Chemistry*, vol. 78, no. 15, pp. 5538–5542, 2006.

[14] P. A. Tran, L. Zhang, and T. J. Webster, "Carbon nanofibers and carbon nanotubes in regenerative medicine," *Advanced Drug Delivery Reviews*, vol. 61, no. 12, pp. 1097–1114, 2009.

[15] L. Z. Swisher, A. M. Prior, M. J. Gunaratna et al., "Quantitative electrochemical detection of cathepsin B activity in breast cancer cell lysates using carbon nanofiber nanoelectrode arrays toward identification of cancer formation," *Nanomedicine: Nanotechnology, Biology, and Medicine*, vol. 11, no. 7, pp. 1695–1704, 2015.

[16] L. Olenic, G. Mihailescu, S. Pruneanu et al., "Investigation of carbon nanofibers as support for bioactive substances," *Journal of Materials Science: Materials in Medicine*, vol. 20, no. 1, pp. 177–183, 2009.

[17] T. D. Nguyen-Vu, H. Chen, A. M. Cassell, R. J. Andrews, M. Meyyappan, and J. Li, "Vertically aligned carbon nanofiber architecture as a multifunctional 3-D neural electrical interface," *IEEE Transactions on Biomedical Engineering*, vol. 54, no. 6, pp. 1121–1128, 2007.

[18] T. Webster, M. Waid, J. L. McKenzie, R. L. Price, and J. U. Ejiofor, "Nano-biotechnology: carbon nanofibres as improved neural and orthopaedic implants," *Nanotechnology*, vol. 15, no. 1, pp. 48–54, 2003.

[19] D. Khang, M. Sato, R. L. Price, A. E. Ribbe, and T. J. Webster, "Selective adhesion and mineral deposition by osteoblasts on carbon nanofiber patterns," *International Journal of Nanomedicine*, vol. 1, no. 1, pp. 65–72, 2006.

[20] E. Gliscinska, B. Gutarowska, B. Brycki, and I. Krucinska, "Electrospun polyacrylonitrile nanofibers modified by quaternary ammonium salts," *Journal of Applied Polymer Science*, vol. 128, no. 1, pp. 767–775, 2013.

[21] A. Fraczek-Szczypta, M. Bogun, and S. Blazewicz, "Carbon fibers modified with carbon nanotubes," *Journal of Materials Science*, vol. 44, no. 17, pp. 4721–4727, 2009.

[22] E. Stodolak-Zych, A. Benko, P. Szatkowski et al., "Spectroscopic studies of the influence of CNTs on the thermal conversion of PAN fibrous membranes to carbon nanofibers," *Journal of Molecular Structure*, vol. 1126, pp. 94–102, 2016.

[23] M. Blazewicz, "Carbon materials in the treatment of soft and hard tissue injuries," *European Cells and Materials*, vol. 2, pp. 21–29, 2001.

[24] I. Rajzer, E. Menaszek, L. Bacakova, M. Rom, and M. Blazewicz, "In vitro and in vivo studies on biocompatibility of carbon fibres," *Journal of Materials Science: Materials in Medicine*, vol. 2, no. 9, pp. 2611–2622, 2010.

[25] E. Dlugon, W. Simka, A. Fraczek-Szczypta et al., "Carbon nanotubes-based coatings on titanium," *Bulletin of Materials Science*, vol. 38, no. 5, pp. 1339–1344, 2015.

[26] A. Abarrategi, M. C. Gutierrez, C. Moreno-Vicente et al., "Multiwall carbon nanotube scaffolds for tissue engineering purposes," *Biomaterials*, vol. 29, no. 1, pp. 94–102, 2008.

[27] A. Neumann and K. Kevenhoerste, "Biomaterials for craniofacial reconstruction," *GMS Current Topics in Otorhinolaryngology-Head and Neck Surgery*, vol. 8, pp. 1–17, 2009.

[28] N. Fanous, A. Tournas, V. Cote et al., "Soft and firm alloplastic implants in rhinoplasty: why, when and how to use them: a review of 311 cases," *Aesthetic Plastic Surgery*, vol. 41, no. 2, pp. 397–412, 2017.

[29] M. Thomas and N. J. Lee, "Interlocking polyetheretherketone implant," *International Journal of Oral and Maxillofacial Surgery*, vol. 45, no. 8, pp. 969-970, 2016.

[30] L. Nayyer, M. Birchall, A. M. Seifalian, and G. Jell, "Design and development of nanocomposite scaffolds for auricular reconstruction," *Nanomedicine: Nanotechnology, Biology and Medicine*, vol. 10, no. 1, pp. 235–246, 2014.

[31] N. Iida, A. Watanabe, and Y. Ando, "Augmentation with hydroxyapatite graft for treating nasal hypoplasia associated with binderoid complete cleft lip," *British Journal of Oral and Maxillofacial Surgery*, vol. 53, no. 7, pp. 666–668, 2015.

[32] K. F. B. Payne, I. Balasundaram, S. Deb, L. Di Silvio, and K. F. M. Fan, "Tissue engineering technology and its possible applications in oral and maxillofacial surgery," *British Journal of Oral and Maxillofacial Surgery*, vol. 52, no. 1, pp. 7–15, 2014.

[33] M. Borrelli, N. Joepen, S. Reichl et al., "Keratin films for ocular surface reconstruction: evaluation of biocompatibility in an in-vivo model," *Biomaterials*, vol. 42, pp. 112–120, 2015.

[34] A. Benko, B. Kolecka, M. Nocun, E. Menaszek, and M. Blazewicz, "CNTs alter the biocompatibility of PAN-derived CNFs," *Engineering of Biomaterials*, vol. 20, no. 143, pp. 71-72, 2017.

[35] I. Rajzer, M. Rom, and M. Blazewicz, "Production of carbon fibers modified with ceramic powders for medical applications," *Fibers and Polymers*, vol. 11, no. 4, pp. 615–624, 2010.

[36] P. Li, I. Kangasniemi, K. de Groot, T. Kokubo, and A. U. Yli-Urpo, "Apatite crystallization from metastable calcium phosphate solution on sol-gel-prepared silica," *Journal of Non-Crystalline Solids*, vol. 168, no. 3, pp. 281–286, 1994.

[37] A. Stoch, W. Jastrzebski, A. Brozek, B. Trybalska, M. Cichocinska, and E. Szarawara, "FTIR monitoring of the growth of the carbonate containing apatite layers from simulated and natural body fluids," *Journal of Molecular Structure*, vol. 511-512, pp. 287–294, 1999.

[38] T. Kokubo and H. Takadama, "How useful is SBF in predicting in vivo bone bioactivity," *Biomaterials*, vol. 27, no. 15, pp. 2907–2915, 2006.

[39] A. Cebulska-Wasilewska, A. Panek, Z. Zabinski, P. Moszczynski, and W. W. Au, "Occupational exposure to mercury vapour on genotoxicity and DNA repair," *Mutation Research/Genetic Toxicology and Environmental Mutagenesis*, vol. 586, no. 2, pp. 102–114, 2005.

[40] A. Cebulska-Wasilewska, I. Pawlyk, A. Panek et al., "Exposure to environmental polycyclic aromatic hydrocarbons: influences on cellular susceptibility to DNA damage (sampling Kosice and Sofia)," *Mutation Research*, vol. 620, no. 1-2, pp. 145–154, 2007.

[41] P. Musiol, P. Szatkowski, M. Gubernat, A. Weselucha-Birczynska, and S. Blazewicz, "Comparative study of the structure and microstructure of PAN-based nano- and micro-carbon fibers," *Ceramics International*, vol. 42, no. 10, pp. 11603–11610, 2016.

[42] A. Stoch, W. Jastrzebski, E. Długon et al., "Modification of carbon composites by nanoceramic compounds," *Journal of Molecular Structure*, vol. 744-747, pp. 627–632, 2005.

[43] A. Stoch, W. Jastrzebski, A. Brozek et al., "FTIR absorption–reflection study of biomimetic growth of phosphates on titanium implants," *Journal of Molecular Structure*, vol. 555, no. 1-3, pp. 375–382, 2000.

[44] Q. Yang, Y. Du, Y. Wang et al., "Si-doping bone composite based on protein template-mediated assembly for enhancing bone regeneration," *Frontiers of Materials Science*, vol. 11, no. 2, pp. 106–119, 2017.

[45] M. Arora and E. Arora, "The promise of silicon: bone regeneration and increased bone density," *Journal of Arthroscopy and Joint Surgery*, vol. 4, no. 3, pp. 103–105, 2017.